

Efficiency enhancement calculations of state-of-the-art solar cells by luminescent layers with spectral shifting, quantum cutting, and quantum tripling function

Citation for published version (APA):

Kate, ten, O. M., Jong, de, M., Hintzen, H. T. J. M., & Kolk, van der, E. (2013). Efficiency enhancement calculations of state-of-the-art solar cells by luminescent layers with spectral shifting, quantum cutting, and quantum tripling function. *Journal of Applied Physics*, 114, 084502-1/9. <https://doi.org/10.1063/1.4819237>

DOI:

[10.1063/1.4819237](https://doi.org/10.1063/1.4819237)

Document status and date:

Published: 01/01/2013

Document Version:

Publisher's PDF, also known as Version of Record (includes final page, issue and volume numbers)

Please check the document version of this publication:

- A submitted manuscript is the version of the article upon submission and before peer-review. There can be important differences between the submitted version and the official published version of record. People interested in the research are advised to contact the author for the final version of the publication, or visit the DOI to the publisher's website.
- The final author version and the galley proof are versions of the publication after peer review.
- The final published version features the final layout of the paper including the volume, issue and page numbers.

[Link to publication](#)

General rights

Copyright and moral rights for the publications made accessible in the public portal are retained by the authors and/or other copyright owners and it is a condition of accessing publications that users recognise and abide by the legal requirements associated with these rights.

- Users may download and print one copy of any publication from the public portal for the purpose of private study or research.
- You may not further distribute the material or use it for any profit-making activity or commercial gain
- You may freely distribute the URL identifying the publication in the public portal.

If the publication is distributed under the terms of Article 25fa of the Dutch Copyright Act, indicated by the "Taverne" license above, please follow below link for the End User Agreement:

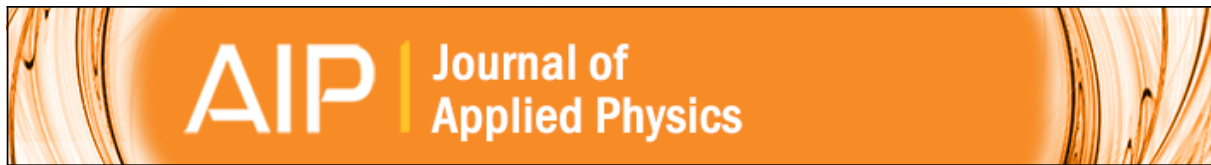
www.tue.nl/taverne

Take down policy

If you believe that this document breaches copyright please contact us at:

openaccess@tue.nl

providing details and we will investigate your claim.



Efficiency enhancement calculations of state-of-the-art solar cells by luminescent layers with spectral shifting, quantum cutting, and quantum tripling function

O. M. ten Kate, M. de Jong, H. T. Hintzen, and E. van der Kolk

Citation: [Journal of Applied Physics](#) **114**, 084502 (2013); doi: 10.1063/1.4819237

View online: <http://dx.doi.org/10.1063/1.4819237>

View Table of Contents: <http://scitation.aip.org/content/aip/journal/jap/114/8?ver=pdfcov>

Published by the [AIP Publishing](#)

Articles you may be interested in

[CuSbS₂ and CuBiS₂ as potential absorber materials for thin-film solar cells](#)

J. Renewable Sustainable Energy **5**, 031616 (2013); 10.1063/1.4812448

[Formation of the physical vapor deposited CdS/Cu\(In,Ga\)Se₂ interface in highly efficient thin film solar cells](#)

Appl. Phys. Lett. **88**, 143510 (2006); 10.1063/1.2190768

[Band alignment at the CdS/Cu\(In,Ga\)S₂ interface in thin-film solar cells](#)

Appl. Phys. Lett. **86**, 062109 (2005); 10.1063/1.1861958

[Enhanced back reflectance and quantum efficiency in Cu\(In,Ga\)Se₂ thin film solar cells with a ZrN back reflector](#)

Appl. Phys. Lett. **85**, 2634 (2004); 10.1063/1.1794860

[Flat conduction-band alignment at the CdS/CuInSe₂ thin-film solar-cell heterojunction](#)

Appl. Phys. Lett. **79**, 4482 (2001); 10.1063/1.1428408



AIP | Journal of Applied Physics

Journal of Applied Physics is pleased to announce **André Anders** as its new Editor-in-Chief

Efficiency enhancement calculations of state-of-the-art solar cells by luminescent layers with spectral shifting, quantum cutting, and quantum tripling function

O. M. ten Kate,^{1,2,a)} M. de Jong,¹ H. T. Hintzen,² and E. van der Kolk¹

¹Luminescent Materials Research Group, Delft University of Technology, Mekelweg 15, 2629JB Delft, The Netherlands

²Energy Materials and Devices, Department of Chemical Engineering and Chemistry, Eindhoven University of Technology, Den Dolech 2, 5600MB Eindhoven, The Netherlands

(Received 10 July 2013; accepted 9 August 2013; published online 23 August 2013)

Solar cells of which the efficiency is not limited by the Shockley-Queisser limit can be obtained by integrating a luminescent spectral conversion layer into the cell structure. We have calculated the maximum efficiency of state-of-the-art c-Si, pc-Si, a-Si, CdTe, GaAs, CIS, CIGS, CGS, GaSb, and Ge solar cells with and without an integrated spectral shifting, quantum cutting, or quantum tripling layer using their measured internal quantum efficiency (IQE) curves. Our detailed balance limit calculations not only take into account light in-coupling efficiency of the direct AM1.5 spectral irradiance but also wavelength dependence of the refractive index and the IQEs of the cells and the angular dependent light in-coupling of the indirect spectral irradiance. An ideal quantum cutting layer enhances all cell efficiencies ranging from a modest 2.9% for c-Si to much larger values of 4.0%, 7.7%, and 11.2% for CIGS, Ge, and GaSb, respectively. A quantum tripling layer also enhances cell efficiencies, but to a lesser extent. These efficiency enhancements are largest for small band gap cells like GaSb (7.5%) and Ge (3.8%). Combining a quantum tripling and a quantum cutting layer would enhance efficiency of these cells by a factor of two. Efficiency enhancement by a simple spectral shifting layer is limited to less than 1% in case the IQE is high for blue and UV lights. However, for CdTe and GaSb solar cells, efficiency enhancements are as high as 4.6% and 3.5%, respectively. A shifting layer based on available red LED phosphors like $\text{Sr}_2\text{Si}_5\text{N}_8\text{:Eu}$ will raise CdTe efficiency by 3.0%. © 2013 AIP Publishing LLC. [<http://dx.doi.org/10.1063/1.4819237>]

I. INTRODUCTION

The main limitation for the efficiency of photovoltaic cells is the mismatch between the solar spectrum and the solar cell response. In a single junction device, only photons with energy equal to the band gap of the solar cell can be used optimally. Photons with higher energy lose their excess energy due to thermalization, while photons with energy lower than the band gap of the solar cell cannot be absorbed at all. An additional loss mechanism for solar cells is that the quantum efficiency for the conversion of each absorbed photon into electricity, called the internal quantum efficiency (IQE), is often lower than 1 due to low exciton diffusion lengths, and rear and front surface recombination. Especially, the front surface recombination limits the IQE of solar cells for the high energy photons.

Several approaches have been suggested in order to solve the spectral mismatch problem, either by adapting the solar cell to the solar spectrum or by adapting the solar spectrum to the solar cell. Examples of the former one are tandem solar cells and multiple exciton generation. The latter approach, adapting the solar spectrum to the solar cell, can conveniently be applied to existing solar cells. A spectral shifting layer on top of a cell can increase the solar cell efficiency by converting high energy photons for which IQE is

low into lower energy photons for which the IQE is high. Furthermore, efficiency can be increased even further, if the conversion layer does not just shift the photons to a lower energy, but in addition cuts each high energy photon into two lower energy photons that still can be absorbed by the solar cell.¹ Such a layer is called a quantum cutting or down-conversion layer.

Since for small band gap cells the efficiency is limited due to large thermalization of the absorbed photons, while for large band gap cells the efficiency is limited due to a reduction in the number of photons that can be absorbed, there will be an optimum in the efficiency as a function of the band gap. This optimum is located at 1.1 eV, as has been calculated by Shockley and Queisser while taking into account the principle of detailed balance.² In the model described by Shockley and Queisser, the solar cell is described as a blackbody radiator that absorbs all light above the band gap of the cell and no light below the band gap. In the calculations, the cell has a refractive index of 1 and operates at a temperature of 300 K under illumination of a blackbody with a temperature of 6000 K (the sun). In the absence of non-radiative recombination, the efficiency reaches a maximum, the so-called Shockley-Queisser limit (SQ-limit), of 31% for a cell with a band gap of 1.3 eV.

Based on the model of Shockley and Queisser, Trupke *et al.*³ calculated the maximum efficiency of solar cells containing a quantum cutting layer. In these kinds of cells, efficiencies above the Shockley-Queisser limit can be obtained,

^{a)}Author to whom correspondence should be addressed. Electronic mail: o.m.tenkate@tudelft.nl

since the thermalization of high energy photons is reduced by cutting a high energy photon into two lower energy photons. Badescu *et al.*^{4,5} extended the model by carefully taking into account the influence of the refractive indices of the different layers on the light in-coupling into the solar cell. Thomas *et al.* recently used these models to calculate the efficiency of a cell with a spectral shifting layer on top.⁶

In this paper, the efficiencies of solar cells containing spectral shifting and quantum cutting layers are calculated based on the models of Trupke and Badescu. However, we extend the model by including the IQE curves of different types of existing state-of-the-art solar cells into the calculations, in order to get an understanding whether, and to what extent, spectral conversion layers would improve the efficiencies of existing solar cells. Additionally, we simulate the solar radiation with the AM 1.5 spectrum instead of pure blackbody radiation of the sun, since the AM 1.5 spectrum better describes the solar radiation and because it is used as a standard for measuring solar cell efficiencies. A third difference with previously published papers is that we do not consider the refractive index of the solar cell as a constant, but instead we take account for the wavelength dependency of the refractive index. Additionally, we consider real spectral shifting, quantum cutting, and quantum tripling materials containing lanthanide ions (Eu^{2+} , Yb^{3+} , Tm^{3+}) as the luminescent centers.

II. THEORY

In Figure 1, a schematic overview of the photovoltaic device that we consider is shown. It consists of the cell itself, which is called medium 4 with on top of it a spectral conversion layer, which is called medium 3. At the rear side of the cell a back-reflector is present, which is assumed to reflect 100% of the light at all wavelengths. The air surrounding the device is called medium 1. Additionally, the cell has an encapsulation layer (medium 2) on top of the conversion layer. This encapsulation layer represents a glass or plastic material that protects the device from the environment. It is considered to be completely transparent for light of all wavelengths with a refractive index of 1.5.

The maximum efficiency η of the photovoltaic device is given by the maximum electrical power per unit area P_e that

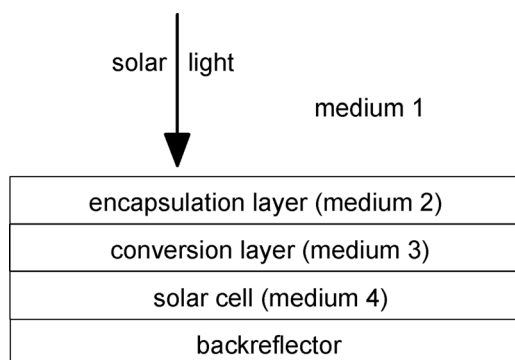


FIG. 1. Schematic overview of the solar cell (medium 4) with a conversion layer (medium 3), encapsulation layer (medium 2) and a back-reflector, surrounded by air (medium 1).

is generated by the cell divided by the solar total irradiance incident on the device P_s , where P_e is equal to the product of the current I and the voltage V at the point where the product is at its maximum

$$\eta = \frac{P_e}{P_s} = \frac{(IV)_{\max}}{P_s}. \quad (1)$$

The solar cell efficiency depends on the spectral irradiance of the light incident on the device. The efficiency is therefore usually determined using two standardized AM 1.5 spectra (ASTM G173-03), which both correspond to a solar zenith angle of 48.2° . The two spectra define a total hemispherical spectral irradiance that includes both the direct and the indirect radiation, and a direct normal spectral irradiance that only includes the direct and circumsolar radiation. In our calculations, the direct normal spectral irradiance Φ_d is described by a Gaussian fit of the standardized direct normal spectrum. A Gaussian fit of the difference between the total hemispherical irradiance and the direct normal irradiance is used to describe the indirect or diffuse spectral irradiance Φ_i . Both fits are shown in Figure 2. In the calculations, it is assumed that the indirect spectral irradiance is uniformly distributed over the hemisphere. The integral of the spectral irradiance over all wavelengths λ gives the solar total irradiance P_s incident on the device:

$$P_s = \int_0^\infty \Phi_d d\lambda + \int_0^\infty \Phi_i d\lambda. \quad (2)$$

In order to get an expression for the current through the cell, expressions are needed for the amount of photons that are absorbed in the cell and the amount of photons that are emitted by the cell. The number of photons that are absorbed in the cell (medium 4) per square meter per second is equal to the sum of three contributions: photons from the direct solar radiation, the indirect solar radiation, and photons emitted by the spectral conversion layer (medium 3).

Only photons with energy higher than the band gap of the solar cell are taken into account, since other photons cannot be absorbed and will not contribute to the current. N_{1d4} , the amount of photons from the direct solar radiation per

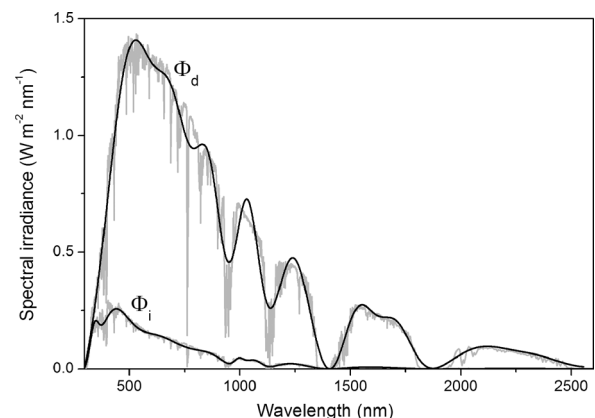


FIG. 2. Gaussian fit (black) and original curve (grey) of the direct normal spectral irradiance Φ_d and the indirect spectral irradiance Φ_i .

square meter per second that are transmitted through the conversion layer and that can be absorbed in the cell and contribute to the current, is equal to

$$N_{1d4} = \frac{1}{hc} \int_0^{\lambda_g} f_{1d4} IQE (1 - \alpha_3) \Phi_d \lambda d\lambda. \quad (3)$$

Here, h is the Planck constant, c the speed of light, λ_g the wavelength that corresponds to the band gap energy E_g and α_3 the spectral fraction of the light absorbed by the spectral conversion layer. f_{1d4} is a factor that describes the fraction of the direct solar radiation that is transmitted via the intermediate layers into medium 4, taking into account the wavelength dependency of the radiation, as well as the refractive indices of the different layers, but neglecting interference effects, as is described in the Appendix. Since a part of the electrons and holes will recombine non-radiatively and therefore not contribute to the current, the factor IQE , which is the internal quantum efficiency of the solar cell, is also included in Eq. (3). It should be noted that this approach is slightly different than the approach followed by Badescu *et al.*⁴ in which efficiency factors were included to account for the carrier generations and recombinations, while in this work these effects are included in the IQE .

Similar as for the direct radiation, the indirect solar radiation N_{1i4} that is absorbed in the cell is equal to

$$N_{1i4} = \frac{1}{hc} \int_0^{\lambda_g} f_{1i4} IQE (1 - \alpha_3) \Phi_i \lambda d\lambda, \quad (4)$$

where f_{1i4} is the factor for the transmittance of the indirect solar radiation into medium 4, as described in the Appendix.

Photons that are absorbed in the conversion layer (medium 3) enter this layer either from medium 1 via medium 2 as direct and indirect solar radiation, or from medium 4 due to radiative recombination in the cell. In practice, the contribution of the latter term can be neglected, since the radiation of the cell is primarily at wavelengths at or just above the band gap of the cell and therefore cannot be absorbed by the conversion layer. The amount of photons that are emitted by the conversion layer is determined by the fraction of the incoming photons that are absorbed α_3 and the quantum efficiency of the spectral conversion η_{em} . The amount of photons leaving the conversion layer is therefore equal to

$$N_{3out} = \frac{1}{hc} \int_0^{\infty} \alpha_3 \eta_{em} (f_{1d3} \Phi_d + f_{1i3} \Phi_i) \lambda d\lambda, \quad (5)$$

where f_{1d3} and f_{1i3} are transmittance factors (see Appendix). All photons emitted by medium 3 have to go either to medium 1 (outside the device) or to medium 4. The amount of photons going to medium 4 and contributing to the current is

$$N_{34} = f_{34} N_{3out} IQE_{av}, \quad (6)$$

where f_{34} is the fraction of the by the conversion layer emitted photons that reach medium 4 (see Appendix) and IQE_{av}

is the average internal quantum efficiency of the solar cell and the energy of the emission of the spectral converter

$$IQE_{av} = \frac{\int_0^{\infty} IQE \cdot I_{em} d\lambda}{\int_0^{\infty} I_{em} d\lambda}. \quad (7)$$

Here, I_{em} is the wavelength dependent emission intensity of the spectral converter. The number of photons emitted by the cell due to radiative recombination depends on the temperature T_c of the cell and the voltage V over the cell and is described by a generalization of Kirchhoff's law of radiation.^{2,3} The photon flux N_{41} for the emission of light from medium 4 via medium 3 and 2 to medium 1 is therefore described by

$$N_{41} = 2\pi n_4^2 c \int_0^{\lambda_g} \frac{1}{\lambda^4} \frac{f_{41} (1 - \alpha_3)}{\exp\left(\frac{(hc/\lambda) - qV}{kT_c}\right) - 1} d\lambda. \quad (8)$$

Here, f_{41} is a factor that accounts for the transmission of light from medium 4 to medium 1 (see Appendix). Note that the factor $(1 - \alpha_3)$ could be omitted since the radiation is primarily at wavelengths that cannot be absorbed by the spectral converter.

The amount of current that can be extracted out of the solar cell is equal to the elementary charge unit q times the amount of minority charge carriers that are collected at the electrodes. The latter is equal to the amount of photons that are absorbed and do not give rise to non-radiative recombination, minus the amount of photons that are emitted by the solar cell. The current through the cell is therefore equal to the sum of the contributions given by Eqs. (3), (4), and (6) minus the contribution given by Eq. (8)

$$I = q(N_{1d4} + N_{1i4} + N_{34} - N_{41}). \quad (9)$$

This current is therefore a function of the voltage V . The maximum efficiency is now given by Eq. (1) at the point where IV is at its maximum.

III. RESULTS AND DISCUSSION

A. Solar cell without spectral conversion layer

If the conversion layer (medium 3) and the encapsulation layer (medium 2) are omitted from the calculations, if the refractive index of the cell (medium 4) is 1, and if the internal quantum efficiency of the cell is 100%, the SQ-limit is obtained, with the difference that Shockley and Queisser simulated the solar spectrum with a blackbody spectrum at 6000 K,² while in these calculations the AM 1.5 spectrum is used. The SQ-limit as a function of the band gap is shown for sake of completeness in Figure 3 and the SQ-limits for some common solar cells are also shown in Table I. The efficiency is at a maximum of 33.5% at 1.15 eV, which is equal to the band gap of the CIGS cell we use in this paper. Also

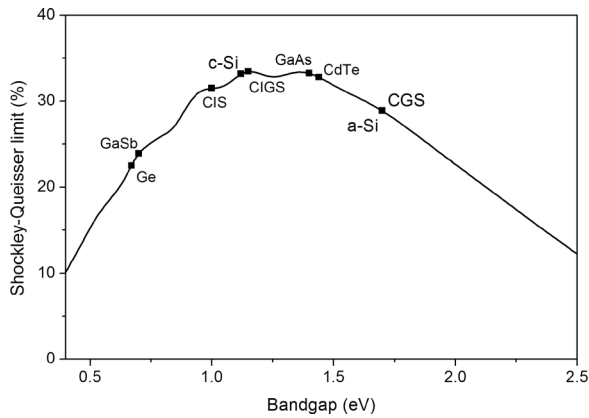


FIG. 3. Shockley-Queisser limit of a solar cell with refractive index of 1 under AM 1.5 solar irradiation as a function of the band gap of the cell. The limits for some frequently used solar cell materials are indicated.

for the band gaps of crystalline silicon (1.12 eV), GaAs (1.4 eV) and CdTe (1.44 eV), the efficiency is close to the optimum value. For small band gap solar cells like GaSb and Ge solar cells, the SQ-limit is considerably lower, due to the large thermalization of the high energy photons in these cells. For solar cells with larger band gaps, the efficiency limit decreases due to a smaller amount of photons that can be absorbed.

In practice, the refractive index of the solar cell will be larger than one, resulting in a less than 100% efficient incoupling of the light, and as a result lower efficiencies. The wavelength dependency of the refractive index for some common solar cell materials is shown in Figure 4. By including these wavelength dependent refractive indices in the calculations, the maximum efficiencies of the solar cells drop significantly, especially for those cells with a relatively high refractive index like c-Si and Ge, as is shown in Table I.

Another loss mechanism for existing solar cells is the fact that the IQE is less than 1 and varies with the wavelength of the light. The short wavelength photons are mainly absorbed in the front part of the solar cell and are therefore strongly affected by surface recombinations, lowering the IQE at the low wavelength side. The long wavelength photons on the other hand are also absorbed in the rear part of

TABLE I. η_{SQ} indicates the SQ-limit for various solar cells with band gap E_g with refractive index of 1 under AM 1.5 solar radiation. η_{ref} is the efficiency limit when the refractive index in Figure 4 is taken into account and η_{iqe} is the efficiency when both the refractive index and the IQE (Figure 5) of the cell are taken into account.

| | E_g (eV) | η_{SQ} (%) | η_{ref} (%) | η_{iqe} (%) |
|-------|------------|-----------------|------------------|------------------|
| c-Si | 1.12 | 33.2 | 21.7 | 19.2 |
| pc-Si | 1.12 | 33.2 | 21.7 | 17.1 |
| a-Si | 1.7 | 28.9 | 17.9 | 14.6 |
| CdTe | 1.44 | 32.8 | 24.4 | 16.3 |
| GaAs | 1.4 | 33.2 | 21.4 | 19.2 |
| CIS | 1.0 | 31.5 | 23.8 | 19.7 |
| CIGS | 1.15 | 33.4 | 24.9 | 21.1 |
| CGS | 1.7 | 28.9 | 20.0 | 15.7 |
| GaSb | 0.7 | 23.9 | 14.6 | 10.1 |
| Ge | 0.67 | 22.5 | 13.2 | 10.5 |

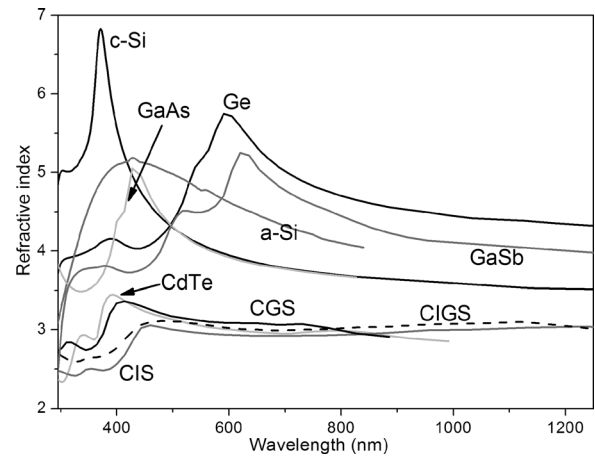


FIG. 4. Refractive index of c-Si,⁷ a-Si (SOPRA Database), GaAs,⁸ CdTe (SOPRA Database), Ge (SOPRA Database), CGS,⁹ CIGS,¹⁰ and CIS.⁹

the solar cell, where rear surface recombinations drop the IQE. In reality, the IQE of one type of solar cell will be different from cell to cell, depending on cell properties like thickness of the layers, and specific processing conditions. Nevertheless, the general shape is the same for one type of cell. Therefore, the IQE curves of some types of solar cells shown in Figure 5, as obtained from literature, are used as the typical IQE curves for these cells in our calculations. The calculated solar cell efficiencies with these IQE curves are shown in Table I. The relative drop in efficiency due to a non-ideal IQE varies from 10% in GaAs to 33% in CdTe.

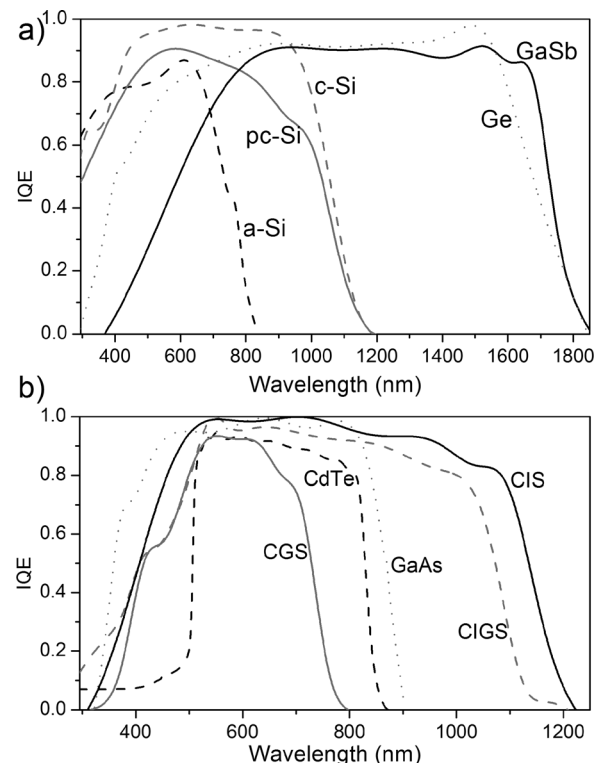


FIG. 5. (a) IQE curves of c-Si,¹¹ thin film pc-Si,¹² a-Si,¹³ GaSb,¹⁴ and Ge¹⁵ solar cells and (b) IQE curves of CdTe,¹⁶ GaAs,¹⁷ CIS,¹⁸ CIGS,¹⁹ and CGS²⁰ solar cells.

B. Spectral shifting layer

Since the IQE, which is shown in Figure 5, decreases at the low wavelength side, a spectral shifting layer positioned on top of the cell which absorbs the low wavelength photons for which the IQE is low and emits photons at a wavelength for which the IQE is at its maximum, could increase the solar cell efficiency. A cell with a single conversion layer and an encapsulation layer, as shown in Figure 1, will be considered and compared with a cell with a non-converting layer with the same refractive index as the conversion layer. This could represent a comparison between a cell with a SiN_x or SiO_x index matching layer that has no or a hypothetical spectral shifting function.

In order to calculate the efficiency of a cell with a spectral shifting layer, four different properties of the spectral shifting layer should be considered: the quantum efficiency of the conversion layer η_{em} , the absorptivity of the layer α_3 , the emission spectrum of the layer I_{em} , and the refractive index n_3 . In the ideal case, the quantum efficiency of the spectral shifting layer is equal to 1 and its emission spectrum is a peak function with the maximum at the wavelength for which the IQE of the cell is at a maximum. The absorptivity α_3 of the spectral shifting layer is, ideally, a step function, being equal to 1 for absorption below a certain absorption edge λ_a and 0 above this wavelength. This corresponds to complete absorption of light below λ_a and no light absorption above λ_a . The properties of an ideal spectral shifting layer can then be found by finding the optimal combination of λ_a and n_3 . These values, along with the corresponding solar cell efficiency, are shown in Table II. The spectral shifting layer will not only enhance the efficiency due to the spectral shifting, but also due to a decrease of the reflectance of the device if the refractive index is in between that of the solar cell and the air. In order to get an understanding of the efficiency increase due to the spectral shifting itself, the efficiencies should be compared with the case in which the device would have a “shifting” layer with the same refractive index, but for which the absorptivity α_3 is 0 for light of all wavelengths, i.e., a transparent layer. These efficiencies η_{transp} are also shown in Table II.

TABLE II. Calculated efficiencies η_{conv} of various solar cells with encapsulation layer ($n = 1.5$) and an ideal spectral shifting layer with an optimal refractive index n_3 , an optimal absorption edge λ_a and an optimal emission wavelength λ_{em} . η_{transp} is the efficiency of a similar cell, but with a transparent layer instead of a conversion layer.

| | λ_{em} (nm) | λ_a (nm) | n_3 | η_{conv} (%) | η_{transp} (%) |
|-------|----------------------------|------------------|-------|--------------------------|----------------------------|
| c-Si | 633 | 474 | 2.3 | 25.7 | 25.3 |
| pc-Si | 648 | 541 | 2.3 | 23.6 | 22.4 |
| a-Si | 611 | 565 | 2.2 | 21.2 | 20.3 |
| CdTe | 552 | 517 | 2.0 | 24.2 | 19.6 |
| GaAs | 640 | 474 | 2.4 | 26.3 | 25.6 |
| CIS | 555 | 475 | 2.1 | 24.6 | 23.7 |
| CIGS | 548 | 515 | 2.2 | 27.2 | 25.6 |
| CGS | 552 | 507 | 2.3 | 22.3 | 19.9 |
| GaSb | 1219 | 811 | 2.4 | 17.4 | 13.9 |
| Ge | 1490 | 1425 | 2.4 | 16.5 | 14.8 |

Table II shows that an ideal spectral shifting layer would be beneficial for the efficiency of all listed solar cells. However, for all cells the efficiency gain is somewhat limited due to the fact that a certain fraction of the light emitted by the conversion layer will be emitted out of the device instead of in the direction of the solar cell. Although the light will be emitted randomly in every direction, this loss factor will not be as high as 50% since the light incoupling in the direction of the cell (which has a higher refractive index) is better than in the direction out of the cell (where the refractive index is lower). However, still circa 15% of the light is lost, which is equal to $1-f_{34}$ as explained in the Appendix. The combination of this loss factor with the fact that the IQE for the silicon solar cells is still relatively high at the low wavelength side explains why the gain in efficiency is only small for the silicon based solar cells. The usefulness of using a conversion layer for silicon solar cells is therefore limited. On the other hand, the CdTe cell would largely profit from a spectral shifting layer with an absolute increase of 4.6% and a relative increase of 23%. The poor IQE below 10% at wavelengths below 450 nm compensates for the fact that about 15% of the converted light is emitted in the wrong direction. A spectral shifting layer would therefore be very beneficial for CdTe solar cells. Note that for the CdTe solar cell, the emission wavelength and absorption edge of the spectral converter do not necessarily have to be exactly at the optimum values as given in Table II. As can be seen in Figure 6, for a large range of values the efficiency will be well above 20% and therefore significantly increase the efficiency of the cell.

Since for some solar cells the efficiency gain is relatively small, even for an idealized spectral shifting material, it is useful to know whether an already existing conversion material would still improve the cell efficiency. As an example, we take a layer made out of an orange-emitting Eu^{2+} doped $\text{Sr}_2\text{Si}_5\text{N}_8$ phosphor, which has a refractive index of 2.55.²¹ This phosphor is known to have a strong absorption in the UV-blue part of the spectrum (see Figure 7) and an efficient emission around 630 nm, depending on the dopant concentration.²²

The $\text{Sr}_2\text{Si}_5\text{N}_8:\text{Eu}$ phosphor is commercially used as conversion phosphor for white LEDs and its efficiency is

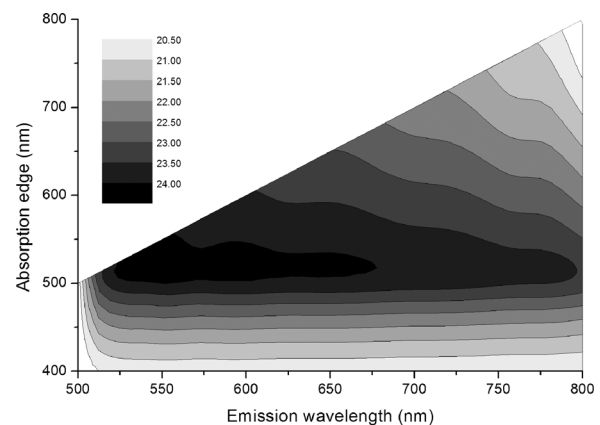


FIG. 6. Calculated efficiencies of a CdTe solar with a spectral shifting layer as a function of the absorption edge λ_a and the emission wavelength λ_{em} .

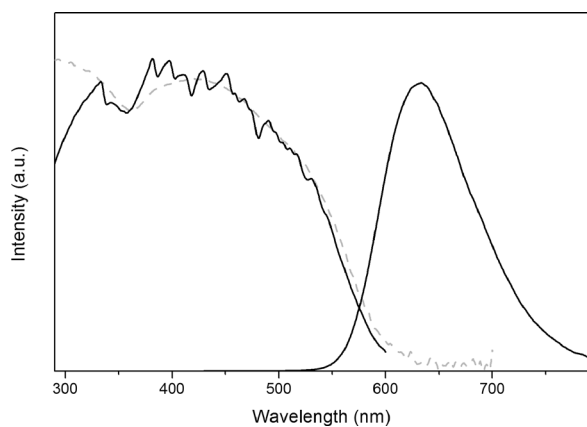


FIG. 7. Absorption (grey line), excitation and emission spectra of $\text{Sr}_2\text{Si}_5\text{N}_8:10\%\text{Eu}$ phosphor.

expected to be around 90%. From Figure 7, it can be seen that the shape of the excitation and the absorption curves are very similar. Therefore, it is assumed that the quantum efficiency is constant over this region. The absorption strength will depend on the thickness of the film. For the calculations, an absorption strength is considered that approaches 100% at 420 nm and drops at longer wavelengths according to the absorption spectrum shown in Figure 7. The emission spectrum of the $\text{Sr}_2\text{Si}_5\text{N}_8:\text{Eu}$ phosphor, as it is used for the calculations, is shown in Figure 7.

The results of the calculations are shown in Table III. For some cells (c-Si, a-Si, CIS, and CIG), the $\text{Sr}_2\text{Si}_5\text{N}_8:\text{Eu}$ conversion layer will decrease the solar cell efficiency as compared to a transparent layer. This can easily be explained, since the efficiency gain was already very small for an ideal conversion layer. In addition, the $\text{Sr}_2\text{Si}_5\text{N}_8:\text{Eu}$ conversion phosphor has a tail in the absorption which extends up to 600 nm. At this wavelength, the IQE of these solar cells is already approaching 100%. Therefore, light that would normally be absorbed in the cell will now be absorbed in the conversion layer. As a result, about 15% of the absorbed light is already lost because it is emitted in the wrong direction and another 10% is lost since the quantum efficiency of the conversion is 90%. Furthermore, for the CGS cell, an additional loss is introduced by the conversion layer: a part of its emission (above 700 nm) is at a wavelength for which the IQE of the CGS is already decreasing.

TABLE III. Calculated efficiencies of various solar cells with a $\text{Sr}_2\text{Si}_5\text{N}_8:\text{Eu}$ conversion layer.

| | η_{transp} (%) | η_{conv} (%) |
|-------|----------------------------|--------------------------|
| c-Si | 25.3 | 25.0 |
| pc-Si | 22.4 | 22.8 |
| a-Si | 20.6 | 19.7 |
| CdTe | 19.3 | 22.3 |
| GaAs | 25.6 | 25.3 |
| CIS | 23.3 | 23.4 |
| CIGS | 25.2 | 25.7 |
| CGS | 19.8 | 19.6 |
| GaSb | 13.9 | 14.9 |
| Ge | 14.9 | 15.1 |

On the other hand, the calculations show that a CdTe or GaSb cell would benefit from the $\text{Sr}_2\text{Si}_5\text{N}_8:\text{Eu}$ conversion layer with absolute gains of 3.0% and 1.0%, respectively.

It should be noted that the $\text{Sr}_2\text{Si}_5\text{N}_8:\text{Eu}$ phosphor used in the calculations is a phosphor that has not been optimized as a spectral conversion phosphor for solar cells. Phosphors for which the emission wavelength, absorption range, and refractive index are optimized for a specific solar cell, would better approach the efficiencies shown in Table II. The $\text{Sr}_2\text{Si}_5\text{N}_8:\text{Eu}$ could, for example, be optimized by the partly substitution of Sr by Ba or Ca or by changing the Eu^{2+} concentration.^{22,23}

C. Quantum cutting layer

One of the main limiting factors for the solar cell efficiency is the thermalization of high energy photons. For photons with energy of more than twice the band gap of the solar cell, more than half of the energy is lost. In silicon solar cells, about 21% of the absorbed photons have an energy of more than twice the band gap and in germanium solar cells this is even 54% of the absorbed photons. One way to solve this problem would be the positioning of a quantum cutting layer on top of the solar cell. In such a layer high energy photons, with an energy of more than twice the band gap, are absorbed, followed by the emission of two photons for each photon absorbed with an energy just above the band gap of the solar cell, which therefore both can be absorbed in the cell.

For solar cells with an IQE of 100%, an ideal quantum cutter would absorb all photons with an energy of $2 E_g$ and above, and emit at a wavelength of exactly $1 E_g$ with a quantum efficiency of 200%. In practice, solar cells have an IQE which decreases at longer wavelengths (see Figure 5). Therefore, cutting the emission to exactly $1 E_g$ will not be optimal. The emission should therefore be at somewhat higher energy. However, the higher the energy of the emission is, the less photons can be cut, so there will be an optimum energy for the emission of the quantum cutting layer.

In Table IV, the results of the calculations are shown for solar cells with a quantum cutting layer of which both the refractive index and the emission wavelength are optimized. Note that for all cells the efficiency is higher than with a normal spectral shifting layer, but that the largest gains are obtained for the low band gap solar cells. For these cells, many photons have an energy of more than $2 E_g$. The solar

TABLE IV. Calculated efficiencies of various solar cells with a quantum cutting layer.

| | η_{transp} (%) | n_3 | λ_{em} (nm) | η_{conv} (%) |
|-------|----------------------------|-------|----------------------------|--------------------------|
| c-Si | 25.3 | 2.4 | 964 | 28.2 |
| pc-Si | 22.5 | 2.4 | 936 | 25.1 |
| CdTe | 19.6 | 2.1 | 814 | 21.7 |
| GaAs | 25.6 | 2.4 | 826 | 27.4 |
| CIS | 23.7 | 2.2 | 1072 | 27.4 |
| CIGS | 25.6 | 2.2 | 1012 | 29.6 |
| GaSb | 13.9 | 2.4 | 1650 | 25.1 |
| Ge | 15.9 | 2.5 | 1514 | 23.6 |

TABLE V. Calculated efficiencies of various solar cells with a Tb³⁺-Yb³⁺ quantum cutting layer.

| | η_{transp} (%) | η_{conv} (%) |
|-------|----------------------------|--------------------------|
| c-Si | 25.3 | 27.6 |
| pc-Si | 22.5 | 24.4 |
| CIGS | 25.6 | 29.1 |

cells with a larger band gap, a-Si and CGS, have not been included in Table V. Their band gaps are too large to be useful in combination with a quantum cutting layer.

For silicon solar cells, a Tb³⁺-Yb³⁺ doped quantum cutting layer has been proposed. In such a quantum cutting material, 485 nm light is absorbed by Tb³⁺ ions and subsequently transferred in one step, via a cooperative energy transfer process, to two neighboring Yb³⁺ ions.¹ Due to the transfer process, the two Yb³⁺ ions are excited in the ²F_{5/2} excited state, and as a consequence will each be able to decay to the ground state of Yb³⁺ with the emission of a 1000 nm photon. Note that this emission is close to the calculated optimal emission wavelength of 950 nm for crystalline silicon solar cells (see Table IV). Also, the optimum emission wavelengths of the CIGS and CIS cells are close to this Yb³⁺ emission.

In practice, the quantum cutting process has some problems that still have to be solved, before a quantum cutting layer could be implemented, such as a poor UV and blue light absorption of the Tb³⁺ ions and the high Yb³⁺ concentration that is needed for an efficient energy transfer process, but that at the same time quenches the Yb³⁺ f-f emission. It is nevertheless interesting to know to what extent a Tb³⁺-Yb³⁺ quantum cutter could improve the efficiency once these problems are solved. In the calculations, we therefore assume that there is no concentration quenching and that the conversion layer contains a sensitizer which efficiently absorbs all light below 485 nm and transfers this energy to the Tb³⁺ ion, which cuts the photons into 1000 nm photons with a quantum efficiency of 200%. The results of the calculations are shown in Table V. The efficiencies are circa 0.5% lower than for the ideal case due to the fact that the Yb³⁺ f-f emission is not exactly at the optimal wavelength and the fact that only light below 485 nm is absorbed, while the light between 485 and 500 nm could also theoretically be cut to 1000 nm photons. However, the efficiencies are still 2 to 3% higher if a Tb³⁺-Yb³⁺ quantum cutting layer is applied.

D. Quantum tripling layer

The advantage of small band gap solar cells is that the absorber materials are able to absorb a large portion of the solar spectrum. However, as a consequence, the energy that is obtained per absorbed photon is limited as a result of the large thermalization of the photons. With a quantum cutting layer, which converts the photons above 2 E_g into two photons of 1 E_g the thermalization is reduced. However, for cells with very small band gaps like germanium or GaSb cells, a part of the solar spectrum will have an energy above 3 E_g. For these cells, a quantum tripling layer, which absorbs the

TABLE VI. Calculated efficiencies of various solar cells with a quantum tripling layer.

| | n_3 | η_{transp} (%) | λ_{em} (nm) | η_{conv} (%) |
|------|-------|----------------------------|----------------------------|--------------------------|
| GaSb | 2.4 | 13.9 | 1662 | 21.4 |
| Ge | 2.5 | 15.9 | 1551 | 19.7 |

photons above 3 E_g and converts each photon into three photons of 1 E_g, could be beneficial. The efficiency calculations for solar cells with a quantum tripling layer are shown in Table VI. Although the efficiencies are a significant improvement compared to a cell with a transparent layer, the efficiencies are lower than for a cell with a quantum cutting (doubling) layer. The reason for this is that less photons can actually be cut if a quantum tripling layer is used, in comparison with a quantum doubling layer, and that the solar spectrum is most intense for those wavelengths that cannot be converted anymore with a quantum tripling layer.

Although the quantum tripling layer appears to be less effective than the quantum doubling layer, one could still make use of the benefit of the quantum tripling process if it is used in combination with a quantum doubling process. The two properties could be combined in one layer, or alternatively in two different layers, where light above 3 E_g is absorbed by the quantum tripler and light between 2 E_g and 3 E_g is absorbed by the quantum doubler. If the two properties are combined in one layer, the efficiencies could increase to the values shown in Table VII. As can be seen, such a combined doubling-tripling layer would largely improve the solar cell efficiency.

An example of a luminescent material that could be used for quantum tripling is a Tm³⁺ doped material, since cross-relaxation can occur between Tm³⁺ ions after excitation in the ¹G₄ level (465 nm) of the Tm³⁺ ion.²⁴ Due to the cross-relaxations, three Tm³⁺ ions can get excited in the ³F₄ level, as is shown in Figure 8. As a result, three 1750 nm photons can be emitted for each photon absorbed. Note that 1750 nm is above the band gap of GaSb and Ge, so in principle these photons can be absorbed by a GaSb or Ge solar cell. However, a higher IQE would be required at that wavelength than the IQE shown in Figure 5, in order to make efficient use of a Tm³⁺ based quantum tripling layer.

Note that for all calculations in this paper, IQE curves are used of solar cells that were published in literature. Therefore, the IQE curves represent cells that were optimized for functioning under AM 1.5 solar irradiation. As an example, crystalline silicon solar cells had an IQE which was relatively poor for UV and blue light irradiation, but years of optimization nowadays result in crystalline silicon solar cells of which the IQE is still relatively good in the UV

TABLE VII. Calculated efficiencies of various solar cells with a conversion layer with both a quantum doubling and quantum tripling function.

| | n_3 | η_{transp} (%) | λ_{em} (nm) | η_{conv} (%) |
|------|-------|----------------------------|----------------------------|--------------------------|
| GaSb | 2.4 | 13.9 | 1648 | 30.5 |
| Ge | 2.5 | 15.9 | 1528 | 28.6 |

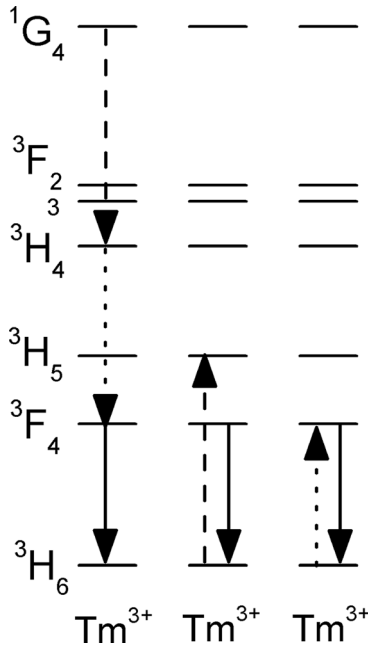


FIG. 8. Tm^{3+} 4f energy levels, showing possible cross-relaxations between three Tm^{3+} ions, resulting in quantum tripling.

and blue. As a result, the efficiency gain by using spectral conversion layers on top of silicon solar cells has decreased. However, for cells with a spectral conversion layer, the optimization of the IQE at low wavelengths becomes unnecessary. Therefore, the extra costs that are needed in order to obtain cells with a high IQE for low wavelengths light could be avoided if a conversion layer is used.

Another point that one should consider is that a conversion layer will also change the efficiency of a cell in another way that is not taken into account in the calculations. Due to the conversion layer, the thermalization of high energy photons will now partly take place in the conversion layer instead of in the solar cell itself, which will probably result in a lower cell temperature. And if the temperature of the cell is lower, the efficiency of the cell will increase, since it will decrease the amount of black body radiation from the cell, as can be seen in Eq. (8).

IV. CONCLUSIONS

We have shown that it is important to include the wavelength dependence of the refractive index and the IQE of solar cells to calculate realistic values for the efficiency enhancement of solar cells by the integration of a luminescent spectral conversion layer. With quantum cutting layers, the efficiency is enhanced for all cells considered and ranges from 2.9% for c-Si to 4.0% for CIGS to 7.7% for Ge. Quantum tripling layers also enhance efficiencies of all cells, especially small band gap cells. However, efficiency enhancements are lower compared to quantum cutting layers due to the smaller amount of photons that can be absorbed by a quantum tripling layer. Combination of the quantum tripling and the quantum cutting layer doubles the efficiency of small band gap solar cells like GaSb or Ge. Efficiency calculations of solar cells with and without a simple spectral shifting layer show that for cells like c-Si, with a

relatively high IQE at the high energy side, the efficiency enhancement is limited and can even lower the efficiency. For other cells that have a low IQE at the short wavelength side, like for example CdTe, the efficiency enhancement is much larger and even the application of available non-optimized spectral shifting materials like $Sr_2Si_5N_8:Eu^{2+}$ can increase efficiency from 19.3 to 22.3%. It would be interesting to take a spectral conversion layer as an integral part of the design and optimization of a solar cell instead of considering such a layer only after the solar cell already has been optimized.

ACKNOWLEDGMENTS

This work is part of the Joint Solar Programme (JSP) of the Stichting voor Fundamenteel Onderzoek der Materie (FOM) and financially supported by HyET Solar.

APPENDIX: CALCULATION OF THE TRANSMITTANCE

The transmittance of an unpolarized light ray from medium a with refractive index n_a to medium b with refractive index n_b as a function of the angle of incidence θ_a can be derived from the Fresnel equations⁴

$$\tau_{ab}(\theta_a) = \frac{2 \cos \theta_a \sqrt{n_{ab}^2 - \sin^2 \theta_a}}{(\cos \theta_a + \sqrt{n_{ab}^2 - \sin^2 \theta_a})^2} + \frac{2n_{ab}^2 \cos \theta_a \sqrt{n_{ab}^2 - \sin^2 \theta_a}}{(n_{ab}^2 \cos \theta_a + \sqrt{n_{ab}^2 - \sin^2 \theta_a})^2}. \quad (A1)$$

Here, n_{ab} is equal to n_b/n_a . Note that this equation is valid for all θ_a if $n_{ab} \geq 1$, but if $n_{ab} < 1$ the equation is only valid if $\theta_a < \arcsin(n_{ab})$. At larger angles $\tau_{ab} = 0$ due to total internal reflection. The transmittance of a light ray from medium a, via medium b, to medium c is given by (neglecting any interference effects)⁴

$$\tau_{ac}(\theta_a) = \frac{\tau_{ab}(\theta_a)\tau_{bc}(\theta_b)}{\tau_{ab}(\theta_a) + \tau_{bc}(\theta_b) - \tau_{ab}(\theta_a)\tau_{bc}(\theta_b)}, \quad (A2)$$

where θ_b is equal to $\arcsin(n_{ab} \sin \theta_a)$. Note that τ_{ac} will be 0 if either τ_{ac} or τ_{bc} becomes 0 due to total internal reflection. If both are 0, Eq. (A2) is not valid and τ_{ac} will be zero as well. Similarly, the transmittance of a light ray from medium a via media b and c to medium d as a function of θ_a is given by

$$\tau_{ad}(\theta_a) = \frac{\tau_{ac}(\theta_a)\tau_{cd}(\theta_c)}{\tau_{ac}(\theta_a) + \tau_{cd}(\theta_c) - \tau_{ac}(\theta_a)\tau_{cd}(\theta_c)}, \quad (A3)$$

where θ_c is equal to $\arcsin((n_a/n_c) \sin \theta_a)$. The geometrical factor B_{ab} for the transmittance of radiation, in case of an axi-symmetrical source of radiation, from medium a to medium b is given by⁴

$$B_{ab} = 2\pi \int_0^\delta \tau_{ab}(\theta_a) \cos \theta_a \sin \theta_a d\theta_a, \quad (A4)$$

where δ is equal to $\pi/2$ in the case of a hemispherical radiation source. When direct solar radiation is considered δ is given by the sine of the radius of the sun ($0.6955 \cdot 10^6$ km) divided over the distance from the sun to the earth ($149.6 \cdot 10^6$ km): 0.00465 rad. The fraction of the spectral radiation that is transmitted from medium a to medium b with respect to the fraction of radiation that can be transmitted when the refractive indices of the layers would be the same, is equal to

$$f_{ab} = \frac{2\pi \int_0^{\delta} \tau_{ab}(\theta_a) \cos \theta_a \sin \theta_a d\theta_a}{2\pi \int_0^{\delta} \cos \theta_a \sin \theta_a d\theta_a} \quad (\text{A5})$$

$$= \frac{2}{\sin^2 \delta} \int_0^{\delta} \tau_{ab}(\theta_a) \cos \theta_a \sin \theta_a d\theta_a.$$

Similarly, the fraction for the transmittance of radiation from medium a via medium b to medium c is equal to

$$f_{ac} = \frac{2}{\sin^2 \delta} \int_0^{\delta} \tau_{ac}(\theta_a) \cos \theta_a \sin \theta_a d\theta_a. \quad (\text{A6})$$

The fraction of the radiation that is transmitted from medium a via media b and c to medium d (f_{ad}) is calculated in a similar way. Radiation emitted by the spectral conversion layer (medium 3) has to be emitted either in the direction of the solar cell (medium 4) or in the direction out of the cell. The transmittance of an unpolarized light ray from medium 3 to medium 4 is then given by

$$T_{34}(\theta_3) = \frac{\tau_{34}(\theta_3)}{\tau_{34}(\theta_3) + \tau_{31}(\theta_3)}. \quad (\text{A7})$$

Therefore, the fraction of the radiation emitted by the conversion layer that is transmitted to medium 4 is

$$f_{34} = 2 \int_0^{\pi/2} T_{34}(\theta_3) \cos \theta_3 \sin \theta_3 d\theta_3. \quad (\text{A8})$$

- ¹P. Vergeer, T. J. H. Vlugt, M. H. F. Kox, M. I. Den Hertog, J. P. J. M. van der Eerden, and A. Meijerink, *Phys. Rev. B* **71**, 014119 (2005).
- ²W. Shockley and H. J. Queisser, *J. Appl. Phys.* **32**, 510 (1961).
- ³T. Trupke, M. A. Green, and P. Würfel, *J. Appl. Phys.* **92**, 1668 (2002).
- ⁴V. Badescu, A. De Vos, A. M. Badescu, and A. Szymanska, *J. Phys. D: Appl. Phys.* **40**, 341 (2007).
- ⁵V. Badescu and A. De Vos, *J. Appl. Phys.* **102**, 073102 (2007).
- ⁶C. P. Thomas, A. B. Wedding, and S. O. Martin, *Sol. Energy Mater. Sol. Cells* **98**, 455 (2012).
- ⁷E. D. Palik, *Handbook of Optical Constants of Solids* (Academic Press, Boston, 1985).
- ⁸D. E. Aspnes and A. A. Studna, *Phys. Rev. B* **27**, 985 (1983).
- ⁹M. I. Alonso, K. Wakita, J. Pascual, M. Garriga, and N. Yamamoto, *Phys. Rev. B* **63**, 075203 (2001).
- ¹⁰M. I. Alonso, M. Garriga, C. A. Durante Rincón, E. Hernandez, and M. León, *Appl. Phys. A* **74**, 659 (2002).
- ¹¹B. Thaidigsmann, A. Wolf, and D. Biro, in *Proceedings of the 24th European Solar Energy Conference and Exhibition, Hamburg, Germany, 21–25 September* (2009), pp. 2056–2059.
- ¹²H. Morikawa, Y. Nishimoto, H. Naomoto, Y. Kawama, A. Takami, S. Arimoto, T. Ishihara, and K. Namba, *Sol. Energy Mater. Sol. Cells* **53**, 23 (1998).
- ¹³J. S. C. Prentice, *Sol. Energy Mater. Sol. Cells* **69**, 303 (2001).
- ¹⁴G. Stollwerck, O. V. Sulima, and A. W. Bett, *IEEE Trans. Electron Devices* **47**, 448 (2000).
- ¹⁵N. E. Posthuma, G. Flamand, and J. Poortmans, in *Proceedings of 3rd World Conference on Photovoltaic Energy Conversion, Osaka, Japan, 18 May* (2003), pp. 777–780.
- ¹⁶M. Hädrich, H. Metzner, U. Reislöhner, and C. Kraft, *Sol. Energy Mater. Sol. Cells* **95**, 887 (2011).
- ¹⁷K. Xiong, S. Lu, T. Zhou, D. Jiang, R. Wang, K. Qiu, J. Dong, and H. Yang, *Sol. Energy* **84**, 1888 (2010).
- ¹⁸J. A. M. Abushama, S. Johnston, T. Moriarty, G. Teeter, K. Ramanathan, and R. Noufi, *Prog. Photovoltaics* **12**, 39 (2004).
- ¹⁹W. K. Metzger and M. Gloeckler, *J. Appl. Phys.* **98**, 063701 (2005).
- ²⁰S. Nishiwaki, A. Ennaoui, S. Schuler, S. Siebentritt, and M. C. Lux-Steiner, *Thin Solid Films* **431**, 296 (2003).
- ²¹H. Lutz, S. Joosten, J. Hoffmann, P. Lehmeier, A. Seilmeier, H. A. Höpfe, and W. Schnick, *J. Phys. Chem. Solids* **65**, 1285 (2004).
- ²²Y. Q. Li, J. E. J. van Steen, J. W. H. Kregel, G. Botty, A. C. A. Delsing, F. J. DiSalvo, G. de With, and H. T. Hintzen, *J. Alloys Compd.* **417**, 273 (2006).
- ²³Y. Q. Li, G. de With, and H. T. Hintzen, *J. Solid State Chem.* **181**, 515 (2008).
- ²⁴A. Jaffrès, B. Viana, and E. van der Kolk, *Chem. Phys. Lett.* **527**, 42 (2012).